30th NENE 2021
September 6 - 9
BLED-SLOVENIA
International Conference Nuclear Energy for New Europe

Film Boiling Simulation Around Cylinder with ANSYS Fluent

Mihael Boštjan Končar
Jožef Stefan Institute
Jamova cesta 39
SI-1000 Ljubljana, Slovenia
mbkoncar@gmail.com

Matej Tekavčič, Mitja Uršič
Jožef Stefan Institute
Jamova cesta 39
SI-1000 Ljubljana, Slovenia
matej.tekavcic@ijs.si, mitja.ursic@ijs.si

ABSTRACT

Two-dimensional simulations of heat and mass transfer around a hot circular cylinder moving at a constant velocity through the water were performed with the ANSYS Fluent computational fluid dynamics code. Presented computational setup is a representation of the TREPAM (CEA, France) experiments, where a hot wire was immersed into a pressurized water at constant velocity. Two-phase flow is modelled with the Volume of Fluid method with the Lee evaporation-condensation model. The model was tuned according to the TREPAM experimental data. Effects of wire temperature, wire diameter, water temperature and free flow velocity on the simulation accuracy, stability and convergence were also investigated.

1 INTRODUCTION

Sodium cooled reactors are one of the candidates for the next generation of fast nuclear reactors. Knowledge of the courses of a hypothetical core melt accident are an important nuclear safety issue. Our focus is on the potential interaction of melt with liquid sodium. In this case a rapid and intense heat transfer interaction between the molten core material and the sodium coolant may lead to a vapour explosion [1]. The processes of vapour explosion phenomenon in sodium are currently under investigation. Due to the nature of liquid sodium (opaqueness, chemical reactivity) the experimental investigation of rapid and intense heat transfer during vaporisation is rather difficult. Therefore, the numerical studies could provide valuable insight into the heat and mass transfer mechanisms. Nevertheless, each numerical simulation, especially multiphase, has to be validated against the experimental data. Because vapour explosions are experimentally widely investigated in water, where stronger pressure loads than in sodium can be expected [2], they can provide a solid basis for validation of numerical models.

In this study we are focusing on the film boiling heat transfer around the melt fragment traveling through the coolant. Benchmark experiments that can be used to mimic the film boiling conditions around melt fragment were conducted in the TREPAM (CEA, France) apparatus [3]. In these experiments the melt fragment is represented by a heated wire moving at a constant velocity through the pressurised water.

The first objective of our research is to investigate the applicability of numerical models in the ANSYS Fluent code to simulate the film boiling conditions around the wire. Two-dimensional simulations of the heat transfer around the wire (representing circular fragment) in two-phase turbulent water flow were conducted. The second objective is to evaluate the effect of boundary conditions, i.e. free flow velocity U_∞, wire temperature T_w, free flow temperature T_∞ and circular wire diameter D, on the accuracy, convergence and stability of the numerical simulation. Simulation results, the heat flux from the wire in particular, were validated with the data from the TREPAM experiment [3]. Experience gained can be used for the future numerical studies of the forced film-boiling conditions around a circular fragment in sodium. Since no experiments are available for sodium, such simulations would provide a solid basis to assess the applicability of the film-boiling correlations that are used in the fuel-coolant interaction codes (e.g. Epstein-Hauser [4]).

2 NUMERICAL MODEL

2.1 Simulated flow conditions with computational domain and mesh

The computational setup is a representation of the TREPAM experiments. Based on our past studies [5] and similarity with the conditions during the core melt down, case 54 from the TREPAM experimental data [3] was selected as a baseline case. Effects of T_w, D, U_∞ and T_∞ were investigated by comparison of cases 53, 48, 61 and 55 against the baseline case. Operating pressure in all of the listed cases is 0.12 MPa, which corresponds to the saturation temperature $T_{sat} = 377$ K. The pressure field is not homogeneous across the domain, therefore $T_{sat}(p)$ was defined as piecewise polynomial (similar as the thermodynamic properties of vapour described in the next paragraph). Detailed description of the individual cases is given in Table 1.

Table 1: Detailed description of the simulated TREPAM cases [3]. Cases are compared to baseline case by quantities written in bold.

Case	D[μm]	$U_\infty \left[\frac{\mathrm{m}}{\mathrm{s}}\right]$	T_w[K]	$T_w - T_{sat}$[K]	T_∞[K]	$T_{sat} - T_\infty$[K]	$q_w \left[\frac{MW}{m^2}\right]$
54	96	2	2300	1992	293	84	18
48	**38**	2	2130	1753	291	86	24
53	100	2	**1780**	1408	294	83	14
55	99	2	1900	1523	**361**	16	9
61	47	**0.2**	2300	1992	303	74	16

Due to the large temperature difference between the subcooled water T_∞ and the hot wire T_w, variable properties dependent on the local temperature were used for the vapour phase (thermal conductivity k_V, density ρ_V, specific heat at constant pressure $c_{p,V}$ and dynamic viscosity μ_V) and for the liquid phase (viscosity μ_L) . As the steam tables are not included in the Fluent code, their properties were defined as the piecewise polynomial. Vapour phase properties were evaluated with the Python library CoolProp (version 6.4.1) in 150 points between T_{sat} and T_w or between T_∞ and T_{sat} for water viscosity, respectively [6]. Then the third-degree polynomial was fitted to these points using the least squares polynomial fit included in the Python NumPy module. During numerical iterations the temperatures in the domain can exceed the prescribed boundaries T_{sat} and T_w (or T_∞ and T_{sat} for liquid water) and yield to non-physical results, therefore beyond the boundaries constant properties were set. The

remaining properties of the liquid phase were assumed as constant and were estimated at the temperature $T_L = \frac{T_\infty + T_{sat}}{2}$.

The predominant physical mechanism in the benchmark experiments is forced convection film boiling. Flow can be characterised by Reynolds number that was defined as:

$$Re_L = \frac{\rho_L U_\infty D}{\mu_L}, \quad Re_V = \frac{\rho_V U_\infty D}{\mu_V}. \tag{1}$$

Assuming a vapour film is thin compared to the wire diameter, a predominant heat transport mechanism is heat conduction, hence the convective heat transfer can be neglected. The thickness of the vapour film can be estimated from the measured heat flux q_w [3] with:

$$\delta_V = k_V \frac{\Delta T_V}{q_w}. \tag{2}$$

The estimated film thickness was used to define the initial condition for the steady state simulation and to determine the appropriate size of the mesh cells in the vapour film. All thermodynamic properties used in the estimation were evaluated at film temperature $T_V = (T_{sat} + T_w)/2$ for the vapour phase and at temperature $T_L = (T_\infty + T_{sat})/2$ for the liquid phase.

Mesh was designed according to the estimated vapour film thickness δ_V prescribed by Eq. (2) for a given case. Figure 1 shows a two-dimensional rectangular computational domain ($36\ D \times 20\ D$) with a solid circular fragment (wire) at the origin. The domain is bounded by five boundary zones, of three types: velocity inlet (inlet, far-field top, far-field bottom), pressure outlet (outlet) and wall boundary (wire wall). For turbulence boundary conditions we assumed the default values recommended by Fluent [7].

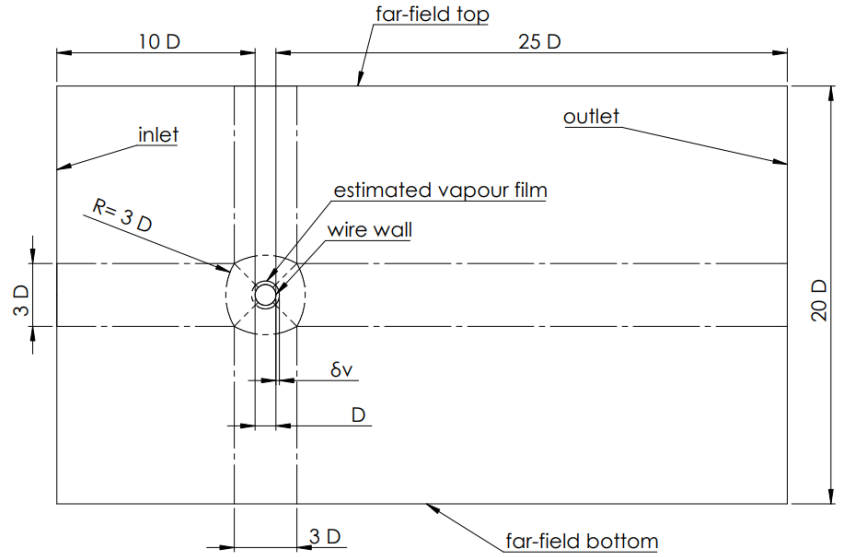

Figure 1: Block structured computational domain with named boundary zones

Block-structured body fitted C-H type mesh with hexahedral cells was used. To better resolve physics in the vapour film additional block was added, i.e. the estimated vapour film zone. Computational cells in the film zone were uniformly distributed in radial direction. Cells around the film zone were then appropriately clustered considering the cell growth factor less than 1.2. Details of mesh configurations used in the simulations are presented in Table 2.

Table 2: Details of mesh configuration

Case number	D[µm]	Re_L	Est. δ_V[µm]	Cells in δ_V (radial dir.)	Total cells
54	96	294	16	28	$1.06 \cdot 10^5$
48	38	112	11	20	$6.31 \cdot 10^4$
53	100	312	10	28	$1.06 \cdot 10^5$
55	99	644	17	28	$1.06 \cdot 10^5$
61	47	17.2	19	20	$6.31 \cdot 10^4$

2.2 Two-phase flow model with heat and mass transfer

The simulations of forced convection boiling were preformed using the implicit formulation of Volume of Fluid model (VOF) with Sharp Interface Modelling in the ANSYS Fluent code [7]. Our past studies have shown that the interface tracking is of great significance when simulating such phenomenon. Namely, the thickness of vapour film in front of the cylinder has the highest impact on the wall heat flux [5].

In all cases the buoyancy effects and gravity can be neglected due to the small geometry and high flow velocities, i.e. if $U_\infty > \sqrt{gD}$ [5]. The requirement is met for all considered cases.

In the flow around a cylinder the transition to turbulence occurs at Re numbers between 150 and 300. The considered Re_L numbers (from 100 to 650) describe the range from laminar to turbulent flow and include the transition region. Since the non-dimensional wall-adjacent grid height y^+ is well below 1 (due to the VOF requirement), the Unsteady Reynolds Averaged Navier-Stokes (URANS) approach with the $k-\omega$ Shear Stress Transport (SST) turbulence model [8] was used for turbulence modelling. It should be noted that most of the available turbulence models are not calibrated for the effects of multiphase turbulence and therefore introduce a source of uncertainty in the simulation.

Surface tension modelling has shown to be important for the stability of the simulation. Effects of surface tension were modelled with continuum surface force model [9]. Due to the high temperature dependency, surface tension coefficient was defined with a piecewise polynomial, similarly to the vapour phase thermodynamic properties based on IAPWS R1-76(2014) [10].

Mass transfer between the liquid and the vapour phase was modelled with the Lee evaporation-condensation model [11] included in the ANSYS Fluent code. The liquid-vapour mass transfer (evaporation and condensation) is governed by the vapour transport equation [7]:

$$\frac{\partial}{\partial t}(\alpha_V \rho_V) + \nabla \cdot (\alpha_V \, \rho_V \, \boldsymbol{u}_V) = \dot{m}_{LV} - \dot{m}_{VL}, \tag{3}$$

where α_V represents vapour volume fraction, ρ_V vapour density and $\boldsymbol{u}_V$ vapour phase velocity. Terms $\dot{m}_{LV}$ and $\dot{m}_{VL}$ represent the mass transfer rates due to the evaporation and condensation, respectively. According to the Lee's model, the mass transfer rate depends purely on the temperature regime and can be described as [7]:

$$\begin{aligned} &\text{if } T_L > T_{sat}\text{: } \dot{m}_{LV} = r \cdot (1-\alpha_V)\rho_L \tfrac{T_L - T_{sat}}{T_{sat}} \text{ (evaporation),} \\ &\text{if } T_V < T_{sat}\text{: } \dot{m}_{VL} = r \cdot \alpha_V \rho_V \tfrac{T_{sat} - T_V}{T_{sat}} \text{ (condensation).} \end{aligned} \tag{4}$$

Term r [s^{-1}] is a coefficient that can be interpreted as relaxation time and determines the intensity of the process. Value of coefficient r is empirical and was one of the main variable

modelling parameters in this study. The source term for the energy equation is obtained by multiplying the rate of mass transfer by the latent heat [7].

2.3 Numerical methods

The forced convection film boiling was difficult to simulate in the transient conditions in terms of numerical stability and convergence, due to a mismatch between the physical model, initial and boundary conditions. To overcome problematic initial transient and gain better initial solution, the simulation was first run in the steady state condition. For the steady state simulations, the coupled method with the pseudo transient relaxation for the pressure-velocity coupling was used. In the transient simulations, the pressure-velocity coupling was performed by the SIMPLE method. Adaptive time step was chosen with the maximum Courant number 0.25 and the minimum time step of 10^{-6} s. Spatial discretisation was performed by the second order upwind scheme for energy and momentum equations and by the first order upwind scheme for all the other equations. It should be noted that the use of the power law scheme instead of the second order upwind scheme in the first iterations was beneficial for the stability and convergence. Simulations of all cases reached a quasi-steady condition and ran well over 100 characteristic time units $\frac{D}{U_\infty}$.

3 RESULTS AND DISCUSION

In the presented study, the primary variable of interest was the area averaged heat flux from the wire wall to the water. This wall heat flux was reported by the Fluent code as output data parameter for each time step in the transient simulation. The data was then arithmetically averaged over the time interval Δt with the Python program routine. Size of $\Delta t = 5 f_s^{-1}$ was estimated from the analogy with the single-phase cross flow over the cylinder, where the shedding frequency is defined as:

$$f_s = \frac{St\, U_\infty}{D}, \tag{5}$$

where St represents the Strouhal number. Empirical correlation used to predict St applicable to the presented cases is formulated as [12]:

$$St = 0.198\left(1 - \frac{19.7}{Re_L}\right). \tag{6}$$

Figure 2 shows the relative error $e_{q,r}$ in the calculation of the heat flux q_{sim} at different values of coefficient r for all presented cases. Evidently, the value of r has a large influence on the magnitude of the wall heat flux, especially in the lower range of r. The simulation results indicate that at high r values, the wall heat flux q_{sim} stabilizes and asymptotically approaches the final value. Furthermore, the value of r directly correlates with the thickness of vapour film δ_V in front of the wire, which inhibits the heat transfer from the wire to the water. As a result, in general, the predicted q_{sim} in the upper range of r is lower than the measured one in the TREPAM experiment. Although the error at higher r values in some cases slightly increases, the use of $r \geq 1000\ \mathrm{s}^{-1}$ is still the most appropriate, as the trend indicates that the final value is within the 50 percent uncertainty for all considered cases. Such accuracy is expected due to the complexity of the physical phenomenon and the numerical models used. It is worth to note, that similar uncertainty (scatter) was also observed when the TREPAM results were compared to the correlations based on the Epstein-Hauser model [13].

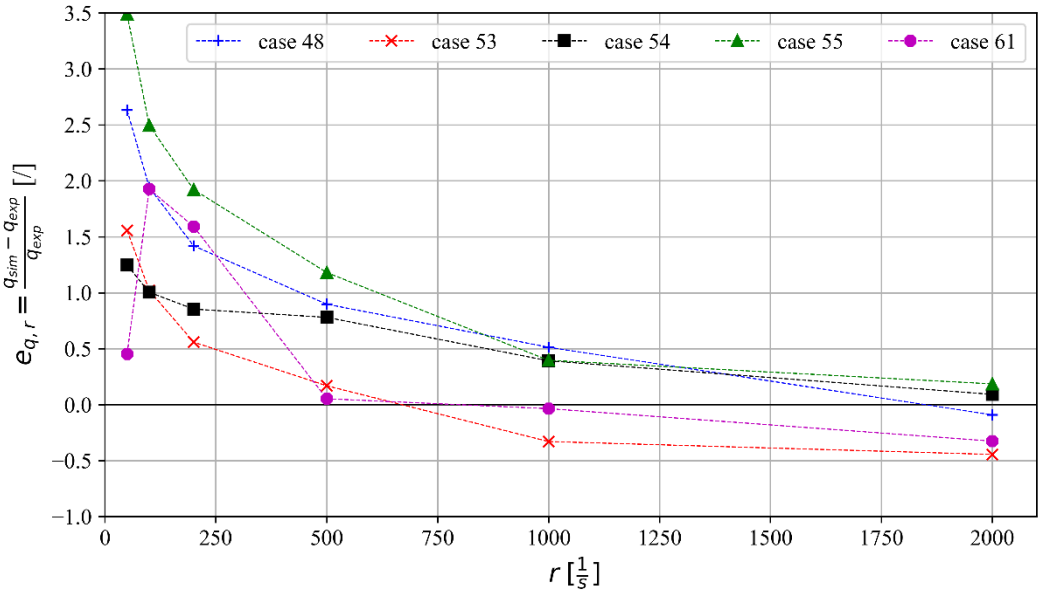

Figure 2: Heat flux relative error vs. value of r in Lee condensation-evaporation model

Comparison between the simulated cases also provides the basis to evaluate effects of boundary conditions on the simulation accuracy. It has been shown that in the cases with higher T_w (cases 48, 54, 55) the use of higher r is required, due to the more intense forced convection boiling. The effect of smaller D is observed in the case 48. In this case the convergence of q_{sim} occurs at higher r compared to the other cases. On the other hand, due to the lower Re, the process is less intense and provides the best agreement ($e_{q,r} = 0$) with experimental results at lower r than the baseline case (case 54). The boundary condition T_∞ has the smallest effect on the simulation accuracy (observed in case 55). It should be noted that due to the small temperature difference between T_∞ and T_{sat}, the simulation of case 55 was considerably less stable than in all other cases with the exception of case 61. The most important variable proved to be U_∞, which is observed in case 61, with ten times lower liquid velocity. The best agreement of q_{sim} with q_{exp} in this case is achieved at significantly lower r than in any other case ($r \in (500\ \mathrm{s}^{-1}, 700\ \mathrm{s}^{-1})$). This could again be a consequence of lower Re and less intense phenomena. However, without experimental evidence it is difficult to determine if such instabilities are either of physical or purely numerical nature. Especially when the fluctuations of q_{sim} for the case 61 are compared with other cases. Comparison with case 55 is shown in Figure 3. It shows major discrepancy that could indicate completely different flow regime or inadequacy of the model. Nevertheless, it has been shown that the simulations with higher U_∞ are much more stable and accurate.

Finally, the Figure 4 shows the comparison of predicted flow regimes for baseline case 54 simulated with two different values of r. Flow regime in the simulation with lower r pose resemblance to the single phase cross-flow around the cylinder with typical up and down movement of the wake behind the obstacle (wire). At higher r, the boiling effects prevail and the flow behind the wire evolves to symmetrical wake with intermittent waves.

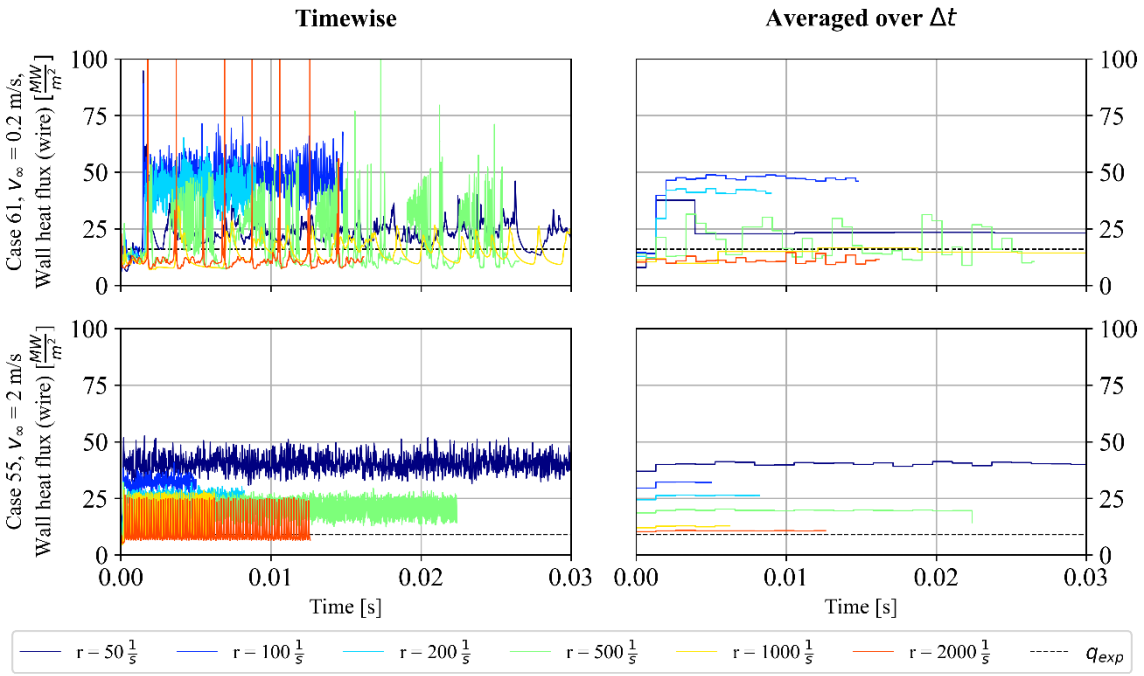

Figure 3: Comparison of wall heat flux time development between case 61 and case 55

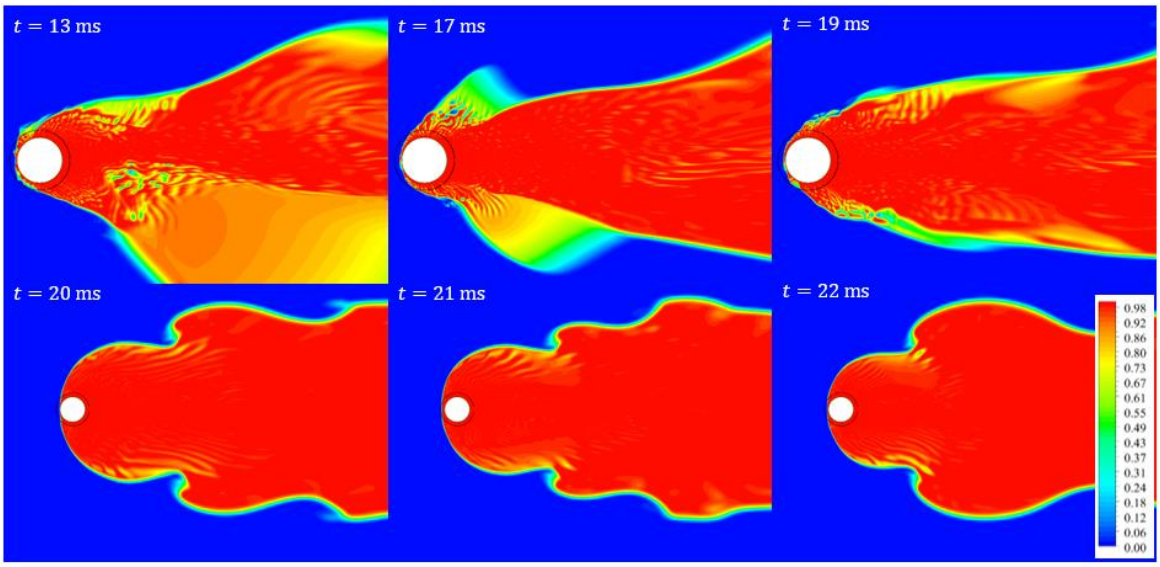

Figure 4: Time development of void fraction in simulations of case 54 with two different value of r, $r = 100\ \mathrm{s}^{-1}$ (upper row) and $r = 1000\ \mathrm{s}^{-1}$ (lower row). Circumference around wire represents estimated vapour film thickness δ_V.

4 CONCLUSION

Simulations of forced convection film boiling of water in saturated liquid conditions are presented. The VOF method was used for interface tracking and the Lee evaporation-condensation model was applied to model the heat and mass transfer around the hot wire. The simulations were validated against the TREPAM experimental data. The results have shown that the most influential parameter in the computational model is coefficient r that determines the intensity of the process in the Lee's model. In all cases, it has been demonstrated that the wall heat flux can be predicted with the reasonable accuracy (within 50 percent) when using

the r value above 1000 s^{-1}. In general, more intense phenomenon (higher wire wall temperature, larger diameter) require higher values of r. The most important parameter for the stability and convergence of the simulation is the free-flow velocity. Namely, a higher velocity stabilises the simulation. In any case, the simulation stability is reduced when the free-flow temperature is close to the saturation temperature. Value of the coefficient r can also affect the flow regime. At lower r, the flow pattern emulates the single phase cross-flow around the cylinder with up down movement of the wake, while at higher r the flow behind the wire evolves to symmetrical wake with intermittent waves.

ACKNOWLEDGMENTS

The authors acknowledge the project (Pressurization process during vapour explosion in sodium cooled fast reactors, J2-8189) and the research core funding No. P2-0026 that were financially supported by the Slovenian Research Agency for the work performed at the Jožef Stefan Institute.

REFERENCES

[1] G. Berthoud, "Vapor explosions", Annu Rev Fluid Mech, 32, 2000, pp. 573-611.
[2] M. Uršič, M. Leskovar, "Investigation of challenges related to vapour explosion modelling in sodium", Nuclear Engineering and Design, 363, 2020, pp. 110646-1-110646-15.
[3] Berthoud G., D' Aillon L. G., "Film boiling heat transfer around a very high temperature thin wire immersed into water at pressure from 1 to 210 bar: Experimental results and analysis", Int J Thermal Science 48, 2009, pp. 1728-1740.
[4] M. Epstein, G. M. Hauser, "Subcooled Forced-Convection Film Boiling in the Forward Stagnation Region of a Sphere or Cylinder", Int J Heat Mass Tran 23, 1980, pp. 179-189.
[5] M. Tekavčič, Ž. Kogovšek, M. Uršič, M. Leskovar, "Simulations of Heat and Mass Transfer Around Circular Core Fragment in Sodium Coolant" Proc. Int. Conf. Nuclear Energy for New Europe 2019, Portorož, Slovenia, September 9-12, Nuclear Society of Slovenia, 2019, pp. 408.1-408.11.
[6] I. H. Bell, J. Wronski, S. Quolin, V. Lemort, "Pure and Pseudo-pure Fluid Thermophysical Property Evaluation and the Open-Source Thermophysical Property Library CoolProp", Industrial & Engineering Chemistry Research 53(6), 2014, pp. 2498-2508.
[7] ANSYS Inc., ANSYS ® Academic Research, Fluent 19 R1, Help System, ANSYS Fluent Theory Guide, 2019.
[8] F. R. Menter, "Two-Equation Eddy-Viscosity Turbulence Models for Engineering Applications", AIAA Journal, 32(8), 1994, pp.1598–1605.
[9] J.U Brackbill, D.B Kothe, C Zemach, "A continuum method for modeling surface tension", Journal of Computational Physics, 100, 1992, pp. 335-354.
[10] IAPWS R1-76. Revised Release on Surface Tension of Ordinary Water Substance, 2014.
[11] W. H. Lee. "A Pressure Iteration Scheme for Two-Phase Modeling", Technical Report LA-UR 79-975, Los Alamos Scientific Laboratory, Los Alamos, 1979.
[12] S. Chandrasekaran, Design of Marine Risers with Functionally Graded Materials, Woodhead Publishing, Cambridge, 2021, pp. 59-90.
[13] R. Meignen, P. S. Picchi, J. Lamome, B. Raverdy, S. C. Escobar, Nicaise, "The challenge of modeling fuel–coolant interaction: Part I – Premixing", Nuclear Engineering and Design, 280, 2014, pp. 511–527.